

Respiratory Rate Estimation from Multi-Lead ECGs using an Adaptive Frequency Tracking Algorithm

Leila Mirmohamadsadeghi, Jean-Marc Vesin

Applied Signal Processing Group, Swiss Federal Institute of Technology, Lausanne, Switzerland

Abstract

Estimating the respiratory rate (RR) from the electrocardiogram (ECG) is of interest as the direct measurement of the respiration in clinical situations is often cumbersome. In this study, the RR was estimated from the multi-lead ECG R-peak amplitude (RPA) waveforms, which contain the modulation of the cardiac activity by the respiration. An adaptive oscillator-based frequency tracking algorithm was used to estimate the RR from the RPAs of two or three ECG leads. This automatic and instantaneous method tracks the common respiratory frequency which is present in its inputs as the RR estimate. On a subset of the Physionet MFH/MF dataset, it was shown that combining information from three leads yielded more accurate RR estimates than using two leads or each lead alone. It was also shown that the frequency tracking algorithm outperformed Fourier-based frequency estimation.

1. Introduction

There is a growing interest in estimating the respiratory rate (RR) from an electrocardiogram (ECG), as the direct measurement of the respiration involves uncomfortable and expensive equipment and on the contrary, the ECG is routinely acquired in clinical and non-clinical situations. Respiration influences the cardiac activity in several ways. In particular, the electric dipole of the heart and the impedance of the thorax change with the respiratory inhalation and exhalation movements. These changes generate a modulation of the ECG R-peak amplitudes (RPA). The RR has already been estimated from the RPA using temporal methods [1], spectral methods [2] and an adaptive method [3]. However, the RPA was shown not to yield accurate RR estimates, which is in part because the suitability of a given ECG lead to represent the respiratory influence is subject-dependent [4]. This variability is caused by the variations in the axis of each lead with respect to the electrical axis of the heart. Often, in ambulatory and clinical applications, multi-lead ECG recordings are available.

Using RPA waveforms derived from several leads may be beneficial in better capturing the respiratory modulation of the ECG amplitude. Multi-lead ECGs have been used to derive the RR by combining RR estimates from four leads in a scheme involving wavelet transfer coherence and a Kalman filter [5]. In the present study, the RR was estimated by using an adaptive frequency estimation algorithm [6] to track the common respiratory frequency in the RPA waveforms of several ECG leads. This algorithm is a weighted multi-signal oscillator-based frequency tracker (W-OSC) that follows a common frequency component in several inputs adaptively and instantaneously. It has been previously applied to the RR estimation from the ECG by using the RPA and the respiratory sinus arrhythmia as inputs [3].

2. Methods

2.1. Data

Evaluation data was a subset of 20 records (total of 41.73 hours of recordings from 7 female and 13 male, aged 49-84 years, with characteristics reported in Table 1) from the Physionet MGH/MF dataset [7] [8]. This dataset was recorded from stable and unstable patients at the Massachusetts General Hospital and contains various physiological recordings of different lengths. The ECG and respiratory impedance recordings are of interest in this study. The selected subset contains leads I, II, an unidentified V lead and the respiratory impedance, digitized at a rate of 360 Hz.

Table 1: Patient characteristics. SR: sinus rhythm, ST: sinus tachycardia, SB: sinus bradycardia, VP: ventricular pacing, AP: atrial pacing, AF: atrial fibrillation, AFL: atrial flutter, JR: junctional rhythm, S: spontaneous, C: controlled, IMV: intermittent mandatory ventilation. The reported values are the RR.

	Cardiac condition	Rhythm	Respiration
mgh005	graft	ST	C 12
mgh006	endocarditis	VP	IMV 8/22

mgh007	graft	SR	S 16
mgh008	endocarditis	AF	S 16
mgh009	graft	ST	IMV 6/20
mgh013	angioplasty	AF	S 20
mgh014	graft	AP	S 18
mgh016	graft	VP	IMV 2/18
mgh020	graft	JR	C 7
mgh024	graft	AFL	S 16
mgh026	graft	ST	S 16
mgh027	carotid endartarectomy	AF	S 18
mgh028	post-infarction angina	VP	S 20
mgh029	graft	ST	C 10
mgh030	none	AF	C 18
mgh031	none	ST	S 30
mgh034	none	SB	S 16
mgh035	graft	SB	IMV 5/8
mgh037	graft	SR	S 16
mgh038	graft	SR	S 16

2.2. RR estimation

For each ECG lead, the RPA waveform was estimated in the following manner: the R-peaks were extracted using maxima detection, the time series of their

amplitudes was then re-sampled uniformly at 2 Hz using cubic spline interpolation and band-pass filtered at respiratory frequencies, i.e., between 0.1 Hz and 0.5 Hz. The RPA waveforms were then fed to the adaptive oscillator-based frequency tracking algorithm individually, then in pairs and finally globally (i.e., all three), yielding ECG-based RR estimates. The respiratory impedance waveform was re-sampled uniformly at 2 Hz using cubic spline interpolation and band-pass filtered between 0.1 Hz and 0.5 Hz. A ground-truth RR estimate was computed from the pre-processed respiratory impedance to assess the accuracy of the estimates resulting from the adaptive oscillator-based frequency tracking algorithm.

2.2.1. Adaptive frequency tracking

An oscillator-based adaptive frequency tracking algorithm (OSC) [6] was used to track the instantaneous frequency of each RPA waveform. This algorithm tracks the frequency of an oscillation. It is based on a band-pass filter, the central frequency of which is adaptively updated by minimizing the error between its output and a perfect oscillation. At each sample, the output of the filter is computed, and used in an adaptive scheme to update the filter such that oscillation criterion is maximized. The multi-input extension of this algorithm, the weighted multi-signal oscillator-based algorithm (W-OSC) [6] was used to adaptively track the common frequency of two or three RPA waveforms. This extension combines the estimates from several inputs by weighting the filter outputs using a scheme based on their signal-to-noise

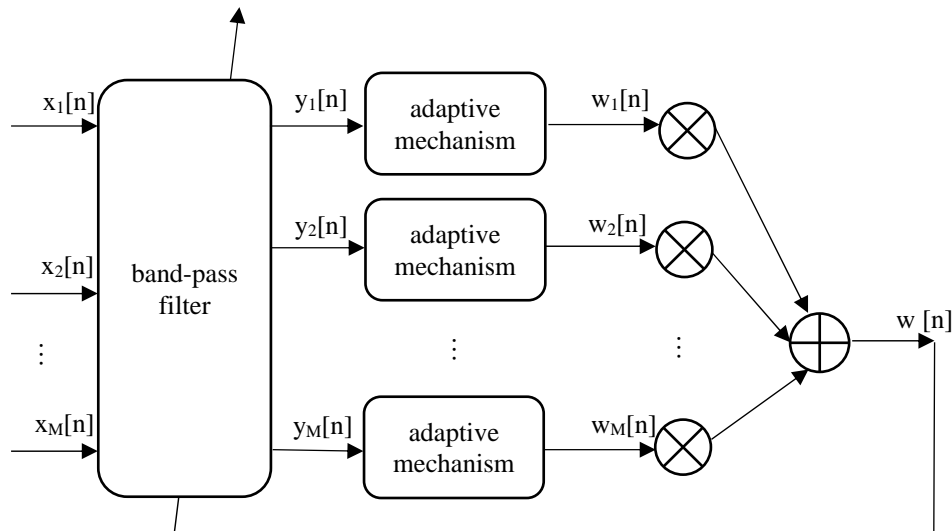


Figure 1: Structure of the W-OSC frequency tracking algorithm. At each sample n , the inputs of the algorithm are denoted as $x_i[n]$, the output of the band-pass filter is denoted as $y_i[n]$ and the frequency estimate of each input is denoted as $w_i[n]$ with $i=1, \dots, M$, where M is the number of inputs. The combination of all estimates yields the final frequency estimate, denoted as $w[n]$. Figure from [9].

ratios as depicted in Figure 1. The W-OSC algorithm was used to estimate the RR using different combinations of two or three RPA waveforms from different leads.

2.2.2. Classic Fourier maximum frequency estimation

A classic Fourier maximum-frequency estimate from the RPA waveform of each lead was computed as well for comparison purposes. The short time Fourier transform was computed with a window length of 28 samples. The frequency corresponding to the local maximum in the Fourier transform was extracted as the reference Fourier frequency estimate.

2.3. Ground-truth

Estimating the ground-truth RR from the respiratory impedance waveform is not a straightforward task as this signal is neither stationary nor necessarily band-limited. In previous studies, the same frequency estimation method applied to the ECG-derived respiratory waveform was used to estimate the ground-truth RR such as in [2]. In the present study, five typical frequency estimates were combined to yield a robust RR ground-truth in order to avoid artificial correlations with the ECG-derived RR estimates as a result of common signal processing methods. The five methods used in this study are the Fourier maximum frequency estimate, the number of respiratory peaks in 20 second-long centered windows, the inverse of the time-lapse between two consecutive respiratory peaks, an estimate based on the Teager-Kaiser energy tracking operator [10], and an estimate based on autoregressive modelling [4]. At each sample, the median of the five estimates and the two estimates closest to it were averaged and low pass filtered to produce the final ground-truth. The accuracy of the ECG-based RR estimates were evaluated by computing their mean absolute error in terms of breaths-per-minute with respect to the ground-truth.

3. Results

Table 2 reports the errors in breaths-per-minute of the OSC estimates for each record and for each lead. Table 3 presents the errors in bpm of the W-OSC estimates using all three leads and different combinations of two leads for each record. Table 4 contains the errors of the Fourier-based estimates on each lead for each record. It was observed that in general, the errors of the W-OSC estimates were the smallest, followed by the OSC estimates. Both W-OSC and OSC estimates had smaller errors than the Fourier-based estimates.

Table 2: The errors in breaths-per-minute of the OSC estimates.

	I	II	V
mgh005	1.75	1.08	2.59
mgh006	9.79	7.61	12.79
mgh007	2.20	2.47	2.86
mgh008	6.10	9.55	9.49
mgh009	6.88	7.03	7.25
mgh013	7.98	9.77	5.31
mgh014	2.66	2.76	3.47
mgh016	4.20	4.14	1.53
mgh020	5.40	1.72	3.75
mgh024	1.05	1.22	0.97
mgh026	4.64	5.00	4.51
mgh027	6.98	9.05	8.27
mgh028	4.97	5.06	5.23
mgh029	5.81	2.73	3.20
mgh030	2.58	1.29	3.45
mgh031	7.06	7.46	6.21
mgh034	4.73	3.89	4.34
mgh035	3.13	4.55	5.93
mgh037	3.09	1.50	2.13
mgh038	2.82	2.78	2.20
average	4.69	4.53	4.77

Table 3: The errors in breaths-per-minute of the W-OSC estimates.

	I,II and V	I and II	II and V	I and V
mgh005	0.61	0.72	0.69	0.78
mgh006	6.74	5.09	6.77	7.97
mgh007	1.65	1.83	1.87	1.79
mgh008	5.60	5.45	6.81	5.69
mgh009	6.04	6.42	5.65	6.94
mgh013	5.46	7.27	4.92	4.86
mgh014	1.80	1.84	2.03	1.95
mgh016	3.01	4.74	2.80	2.08
mgh020	1.88	1.89	1.69	2.75
mgh024	0.87	0.89	0.91	0.90
mgh026	3.05	3.33	3.21	3.21
mgh027	4.75	5.58	5.21	4.92
mgh028	3.68	4.07	3.76	3.62
mgh029	1.14	1.25	1.10	1.23
mgh030	0.83	1.01	0.95	1.10
mgh031	6.09	6.25	6.39	5.72
mgh034	2.88	2.96	2.96	2.95
mgh035	1.52	1.42	1.54	1.57

mgh037	1.36	1.73	1.16	2.21
mgh038	1.82	2.28	1.87	1.94
average	3.04	3.30	3.11	3.21

Table 4: The errors in breaths-per-minute of the Fourier estimates.

	I	II	V
mgh005	2.65	1.28	1.38
mgh006	7.85	5.69	11.10
mgh007	3.16	3.40	3.13
mgh008	9.40	12.00	12.27
mgh009	11.16	6.97	8.90
mgh013	11.05	12.70	8.11
mgh014	3.82	2.58	4.11
mgh016	6.73	6.52	2.39
mgh020	3.02	2.04	3.02
mgh024	1.11	1.45	1.03
mgh026	6.32	5.66	5.50
mgh027	5.59	6.84	6.57
mgh028	4.91	5.20	5.36
mgh029	2.64	1.29	1.36
mgh030	4.30	2.59	3.57
mgh031	11.01	11.74	7.46
mgh034	4.54	3.75	4.37
mgh035	1.66	1.75	2.91
mgh037	4.10	2.54	2.77
mgh038	4.81	4.84	3.47
average	5.49	5.04	4.94

4. Discussion and conclusions

In our study, we have shown that the W-OSC adaptive frequency tracking algorithm using two or three ECG leads yields the most accurate RR estimates as compared to those of the OSC algorithm and Fourier estimates on one lead. The baseline drift of the ECG recordings was not removed, as in this particular case, patients lay still on beds and removing the baseline would remove the respiratory activity, which was of interest in this study. The limitations of this study lie in the small number of patients and the diversity of their health conditions. However, this diversity may also be a strength in demonstrating the feasibility of using the W-OSC algorithm when the patient suffers from a cardiac condition or an abnormal cardiac rhythm. It is possible

that using several leads overcomes one of the limitations of the RPA to estimate the RR, which is the fact that the lead reflecting most the respiratory modulation of the ECG R-peak amplitudes varies among subjects [4]. It would be of interest to investigate the use of more than three leads. The W-OSC algorithm is instantaneous, meaning that it can deliver RR values in real-time. Furthermore, the algorithm is automatic and does not require special treatment to remove abnormal beats as it can rectify their effect within a few iterations.

Acknowledgements

This work was funded thanks to the Swiss NanoTera initiative, RTD project ObeSense.

References

- [1] Cysarz, Zerm R, Bettermann H, Frühwirth M, Moser M, Kröz M. Comparison of respiratory rates derived from heart rate variability, ECG amplitude, and nasal/oral airflow. *Ann Biomed Eng.* 2008;36:2085–2094.
- [2] Orphanidou C, Fleming S, Shah S, Tarassenko L. Data fusion for estimating respiratory rate from a single-lead ECG. *Biomed Signal Process Control* 2013;8:98–105.
- [3] Mirmohamadsadeghi L, Vesin JM. Respiratory rate estimation from the ECG using an instantaneous frequency tracking algorithm. *Biomed Signal Process Control* 2014;14:66–72.
- [4] Bailón R, Sörnmo L, Laguna P. In: Clifford G, Azuaje F, McSharry P, editors. *ECG- Derived Respiratory Frequency Estimation. Advanced Methods and Tools for ECG Data Analysis.* Norwood, MA, USA: Artech House; 2006. .
- [5] Johnson A, Cholleti S, Buchman T, Clifford G. Improved respiration rate estimation using a Kalman filter and wavelet cross-coherence. *Computing in Cardiology* 2013;40:791–794.
- [6] Prudat Y, Vesin JM. Multi-signal extension of adaptive frequency tracking algorithms. *Signal Process.* 2009;89:963–973.
- [7] Welch J, Ford P, Teplick R, Rubsam R. The Massachusetts General Hospital-Marquette Foundation hemodynamic and electrocardiographic database—comprehensive collection of critical care waveforms. *J Clin Monit* 1991;7:96–97.
- [8] Goldberger A, Amaral L, Glass L, Hausdorff J, Ivanov P, Mark R, et al. *PhysioBank, PhysioToolkit, and PhysioNet: Components of a new research resource for complex physiologic signals.* *Circulation.* 2000;101:215–220.
- [9] Van Zaen J. *Efficient schemes for adaptive frequency tracking and their relevance to EEG and ECG.* Ecole Polytechnique Fédérale de Lausanne (EPFL); 2012.
- [10] Potamianos A, Maragos P. A comparison of the energy operator and the Hilbert transform approach to signal and speech demodulation. *Signal Process.* 1994;37:95–120.

Address for correspondence:

Leila Mirmohamadsadeghi
EPFL SCI STI JMV – ELD 234 – Station 11
1015 Lausanne, Switzerland